Diagenesis, regular growth and records of seasonality in inoceramid bivalve shells from mid-Maastrichtian hemipelagic beds of the Bay of Biscay

J.J. Gómez-Alday[1] & J. Elorza[1]

[1] Departamento de Mineralogía-Petrología, Universidad del País Vasco,
Apartado 644, E-48080 Bilbao, Spain; e-mail: nppelzaj@lg.ehu.es

Abstract

Inoceramid bivalve shells from outcrops of mid-Maastrichtian deep-water carbonate, hemipelagic beds in the Bay of Biscay exhibit post-depositional diagenetic alteration. New data from isotopic analysis (carbon and oxygen), together with observations of the inoceramid shells and carbonate host-rock using cathodoluminescence (CL) and scanning electron microscopy (SEM), confirm a lateral, westerly increase in the degree of diagenesis, without any substantial textural changes in the alternating dark and clear growth lines of the shell microstructure. Under CL, a bright yellowish to red colour is observed in the most diagenetically altered inoceramid samples. Non-luminescent areas are restricted to the central parts of the less altered shells. A detailed geochemical analysis by electron microprobe, along intrashell profiles of the non-luminescent and luminescent zones has revealed that Mg/Ca, Sr/Ca, Na/Ca, Fe/Ca and Mn/Ca ratios show oscillatory curves but behave differently. Fe/Ca, Mn/Ca and Na/Ca ratios are well correlated but usually show an opposite relationship when compared with the Mg/Ca and Sr/Ca ratios of both luminescent and non-luminescent shell areas. Our findings have palaeoenvironmental implications in that the geochemistry of the regular, alternating dark and clear growth lines seems to be related to the input of seasonally controlled phytodetritus to the basin floor.

Introduction

Inoceramid bivalves are important Cretaceous biostratigraphical indices because of their cosmopolitan distribution (Dhondt, 1992). Deep Sea Drilling Project (DSDP) studies have revealed that inoceramids occurred in all of the world oceans, at different depths (from shelf to abyssal palaeodepths) and from tropical to austral palaeolatitudes during the Late Cretaceous (Saito & Van Donk, 1974; Saltzman & Barron, 1982; Barron et al., 1984; MacLeod et al., 1996). Inoceramids were epifaunal, filter-feeding bivalves which are found associated with different carbonate or terrigenous sediment substrates.

A variety of comparative geochemical studies (analyses of stable isotopes, and minor and trace elements) of extant as well as different macro- and microfossil calcareous skeletons have been published since the 1980s. Morrison & Brand (1984, 1988), Veizer et al. (1986), Krantz et al. (1987), Barrera & Tevesz (1990) and Barrera et al. (1990), among others, characterised palaeoenvironmental features at different latitudes and sedimentary settings. Studies of minor and trace element contents in the calcareous skeletons of both fossil (Ragland et al., 1979; Brand & Veizer, 1980; Brand & Morrison, 1987; Barbin et al., 1995; Mii & Grossman, 1994; Grossman et al., 1996; Dauphin et al., 1996; Purton et al., 1999) and living

specimens have been published (Morrison & Brand, 1986; Barbin et al., 1991a, b; Mann, 1992; Klein et al., 1996a, b, 1997; Jones & Quitmyer, 1996). It is generally assumed that the final composition of fossil shells is determined by:

A - the physical/chemical environment in which the organism lived;

B - biological controls during skeletal growth; and

C - subsequent diagenetic alteration undergone by the shell (Dodd & Stanton, 1981).

We have previously characterised the diagenetic behaviour of inoceramid shells (paths of diagenetic fluid advance, oxygen and carbon isotope variations, geochemical relationship with the carbonate host-rock, etc.) during progressive burial of Upper Cretaceous sediments in the Basque-Cantabrian Basin (Elorza & García-Garmilla, 1996, 1998; Gómez-Alday & Elorza, 1998), in the chalk facies from the Liège-Limburg basin (Belgium, the Netherlands) (Elorza et al., 1997) and in France (Gómez-Alday et al., 1998). Our first objective was to determine the degree of diagenetic alteration of the new inoceramid samples collected from different sections of the Bay of Biscay from a geochemical and petrographic point of view, and to establish if there are petrographic and geochemical differences between the more altered and the less altered inoceramid shells. In order to evaluate the degree of diagenesis, we examined the inoceramid shells together with the host-rock, under microscopy, SEM and CL. In addition, oxygen and carbon isotopes were determined and the Mg, Ca, Mn, Fe, Sr and Na contents of selected inoceramid shells were also examined. Our second objective was to determine if the less altered inoceramid samples preserve part of the primary palaeobiotic signal and geochemically determine their regular seasonal growth pattern in deep-water environments. In the present paper, we put forward evidence which indicates that certain geochemical values may be close to the original composition (minor and trace elements) of deep-water ocean inoceramid shells.

Geological setting

The Sopelana I, Zumaya, San Sebastián, Hendaya, Loya and Bidart sections are located in the so-called Basque Arc domain (Rat, 1959; Feuillée & Rat, 1971) (see Fig. 1). They comprise well-exposed, Upper Cretaceous sediments, which crop out along the coast of the Bay of Biscay (Spain and France). The samples selected for this study belong to mid-Maastrichtian carbonate-rich facies, which consists of marl and marly-limestone alternations, each about 20-30 cm thick. The occurrence of terrigenous sediments such as distal turbidite beds are important in the Zumaya, San Sebastián, Loya and Hendaya sections (Fig. 2). On the basis of its trace fossil association, benthic forams and ostracods (see Pujalte et al., 1998), the basin has been considered to be mesobathyal (1,500-2,000 m).

Five lithostratigraphic members were recognised within the mid-Maastrichtian of the Zumaya-Algorri Formation (MacLeod & Ward, 1990; Ward & Kennedy, 1993) although with different thickness in the Sopelana I, Zumaya and Bidart sections (this formation was defined by Mathey, 1982, p. 135; and later erroneously referred to by other authors as the Zumaya-Algorta Formation). Inoceramids are most abundant in the so-called Member I, belonging to the *Gansserina gansseri* Zone, and do not reach into the *Abathomphalus mayaroensis* Zone (planktonic forams). They eventually disappear in the upper part of Member II, coinciding with nannofossil zones 24-25A, and equating with the *Anapachydiscus fresvillensis* ammonite zone, in magnetochron 31N (data summarised by MacLeod & Orr, 1993; Ward & Kennedy, 1993) (see Fig. 2).

These lithologically homogeneous sediments were deposited in a hemipelagic environment, which persisted during the Maastrichtian (Mathey, 1982, 1987). Six different species of inoceramids have been identified (MacLeod & Ward, 1990; Ward et al., 1991; MacLeod, 1994). Most inoceramid shells appear
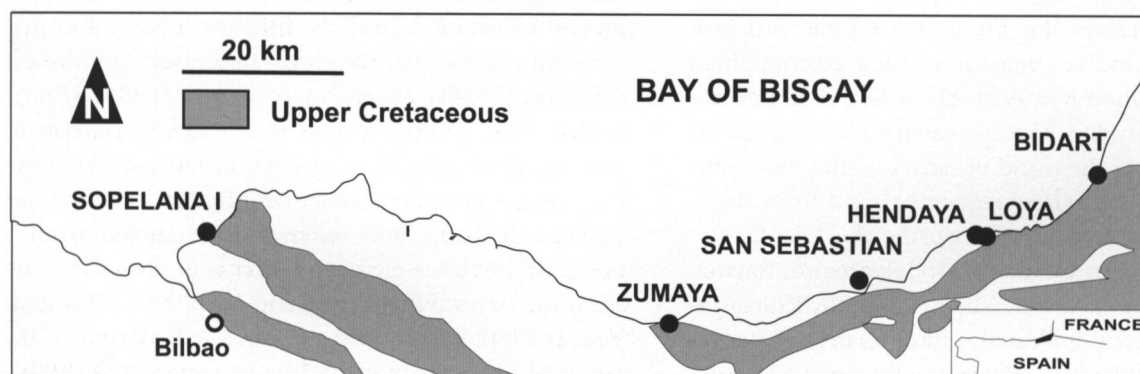

Fig. 1. Map showing localities referred to in the text, and the areal extent of Upper Cretaceous strata.
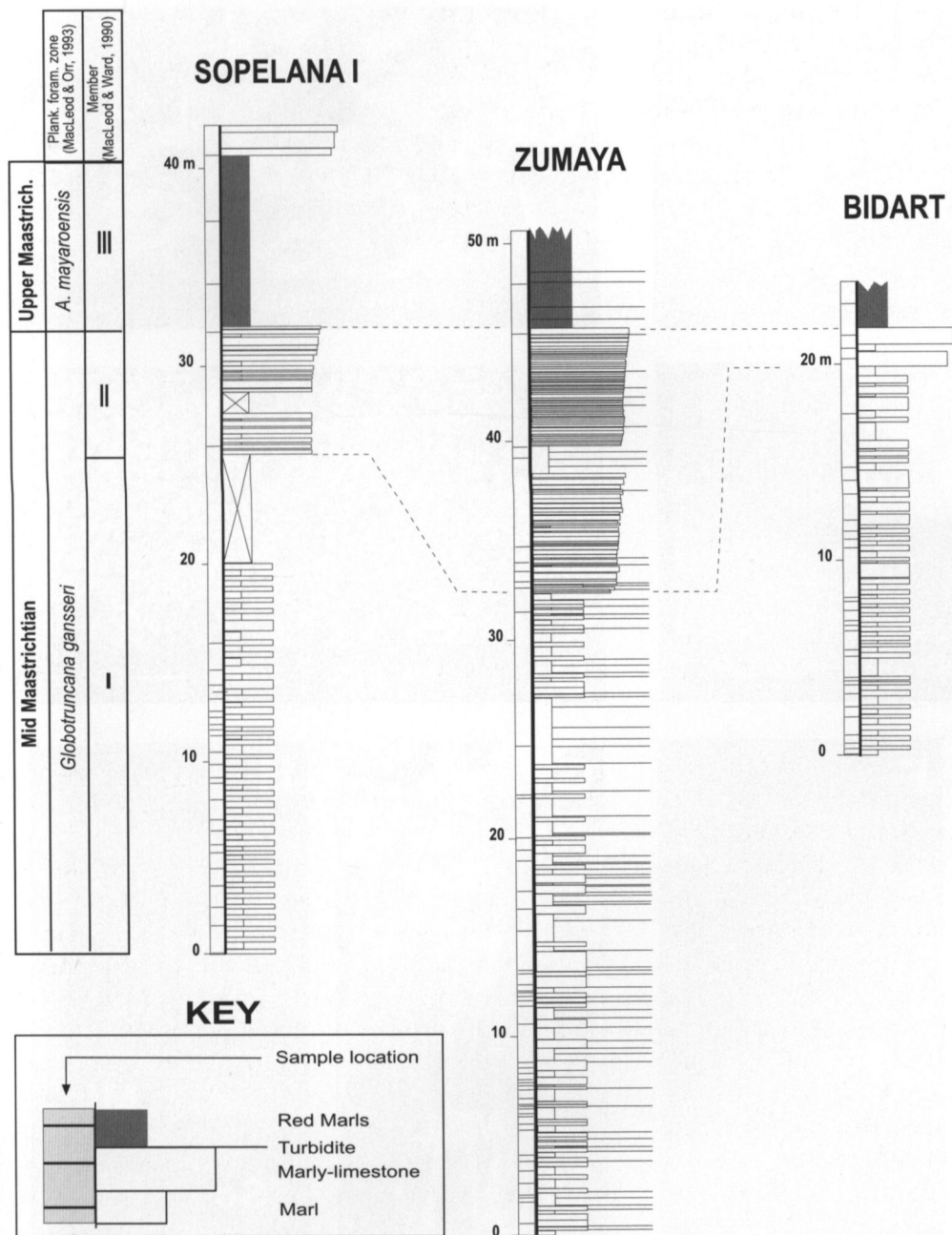
Fig. 2. Stratigraphic logs for the Sopelana I, Zumaya and Bidart cliff sections, showing the various lithostratigraphic members (I-III), planktonic foraminiferal zones (*Globotruncana gansseri* [= *Gansserina gansseri*] and *Abathomphalus mayaroensis*) and the location of inoceramid samples collected together with the carbonate host-rock.

complete both in marly and marly-limestone sediments. Sometimes, they are colonised by small oyster shells (*Pycnodonte* sp.). Small, oriented, comma-shaped borings can also be observed which correspond to cirripede endobionts such as *Rogerella*, and are mainly distributed following the dark growth lines.

Methods and materials

Fragments of inoceramid prismatic calcite shell material were selected and examined under SEM using a Jeol JSM-T6400 at the Universidad del País Vasco. All CL work employed a Technosyn Cold Cathode Luminescence system, model 8200 Mk II, mounted on an Olympus trinocular research microscope with a maximum magnification capability of x400, utilising universal stage objectives. Standard operating conditions included an accelerating potential of 12 kV and a 0.5-0.6 mA beam current with a beam diameter of approximately 5 mm.

The selected samples from the six stratigraphic sections were analysed for oxygen and carbon isotopes. The stable isotope values of $^{18}O/^{16}O$ and $^{13}C/^{12}C$ from inoceramid shells and host-rock were determined by using a VG SIRA-9 mass spectrometer at the Universidad de Barcelona and Universidad de Salamanca (Spain). Extraction of CO_2 from carbonates was carried out according to the McCrea method (1950). The results are expressed in ∂ notation in ‰, relative
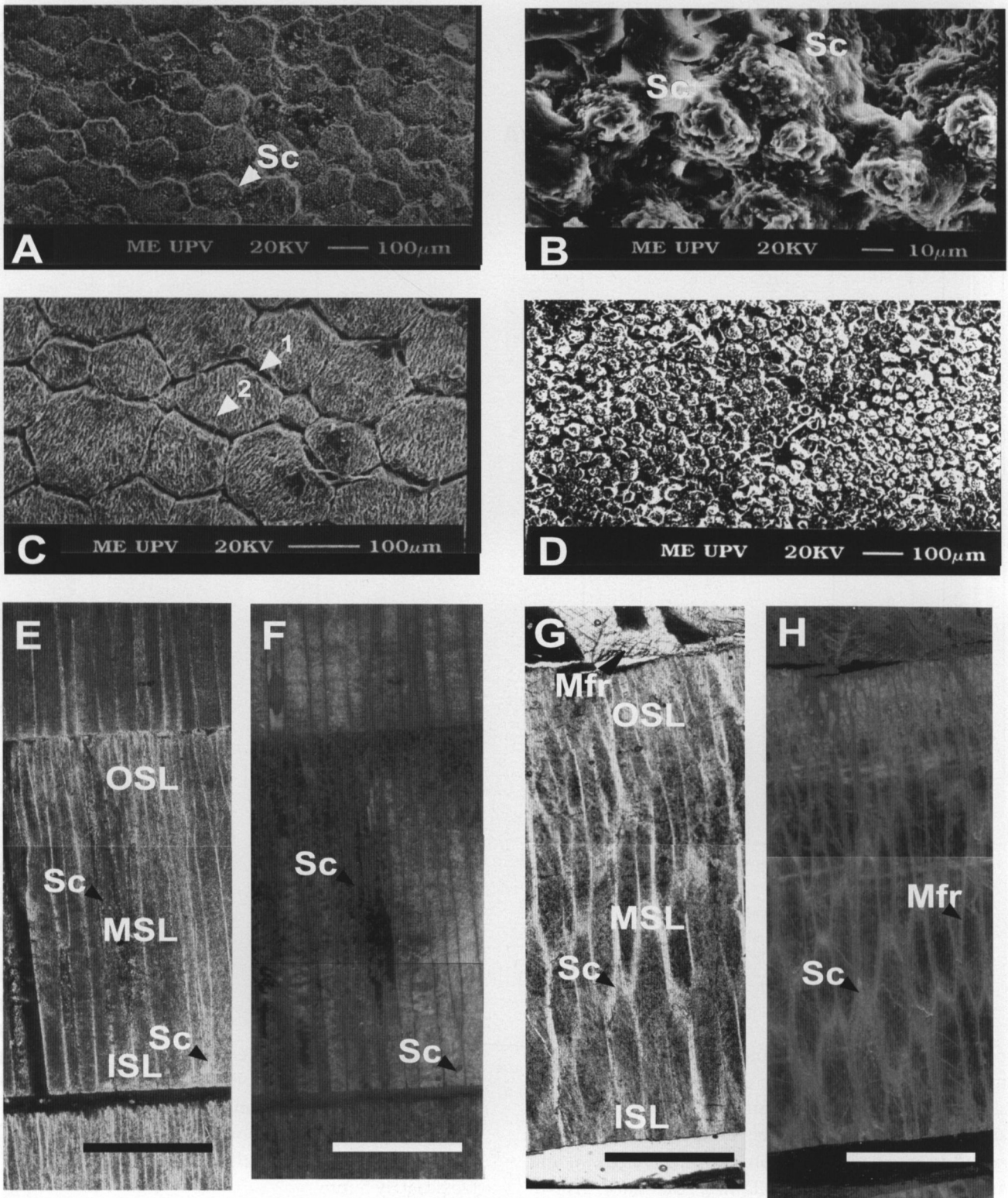
Fig. 3. Inoceramid shell photomicrographs under SEM (A-D), transmitted light (E, G) and cathodoluminescence (F, H). In spite of the fact that the MA-33 inoceramid shell exhibits a well-defined 'honeycomb' microstructure in the ISL (A), the inter- and intraprism microporosity is not preserved due to the precipitation of secondary calcite (Sc). This feature contrasts with that seen in the BID-1 inoceramid shell (C), in which primary porosity is well preserved (arrows 1 and 2). The same process can be ascribed to the small prisms of the MA-33 (B) and BID-1 (D) OSL surfaces. When the degree of secondary calcite precipitation is significant, it can lead to a marked $\partial^{18}O$ depletion. This is the case in the Hendaya (HE-2) and Loya (LO-5) samples (E-H). The HE-2 (E, F) and LO-5 (G, H) inoceramid samples show interprism zones filled with diagenetic calcite. A fracture crossing the host rock is observable in the upper part of G. Abbreviations: Mfr - microfracture; OSL - outer shell layer; MSL - middle shell layer; ISL - inner shell layer.

to the Pee Dee Belemnite (PDB) standard. Reproducibility for both $\partial^{18}O$ and $\partial^{13}C$ is better than 0.1‰.

In addition, the inoceramid shell samples MA-33 (Sopelana I section) and BID-1 (Bidart section), which have the lightest and heaviest oxygen isotope values, respectively, and distinct CL were polished to determine the Mg, Ca, Mn, Fe, Sr and Na contents by electron microprobe. A Cameca SX100 electron microprobe at the Département des Sciences de la Terre (Université Blaise Pascal, Clermont-Ferrand, France) was used for this purpose. Working conditions were 10 s counting time, *c.* 10 nA beam current and 15 kV accelerating voltage, using a beam area of 20 μm^2. Calibration was against Bureau de Recherches géologiques et minières (BRGM) standard minerals, and the ZAF correction program was used (Henoc & Tong, 1978). The analyses in shells (a total of 277 spots) were performed taking into account the thickness of the growth lines; where it was not possible to recognise them, sampling was carried out at

20 μm intervals, which is the usual distance between two consecutive growth lines. During analyses, we tried to avoid the longitudinal inter-prism surfaces due to their potential ways of diagenetic calcite precipitation. In order to facilitate comparison with other studies, the chemical composition of inoceramid shells was also recalculated as ppm of Mg, Ca, Mn, Fe, Sr and Na.

Results

Petrography of inoceramid shells

More than 100 thin sections were examined by standard microscopy methods. These sections were stained with Alizarin Red S and potassium ferricyanide (Dickson, 1965). A well-developed, prismatic calcite microstructure characterises the inoceramid shells, which range from 1 to 6 mm in thickness (Figs 3A-H, 4A, 6A, B). In longitudinal shell sections, cal-
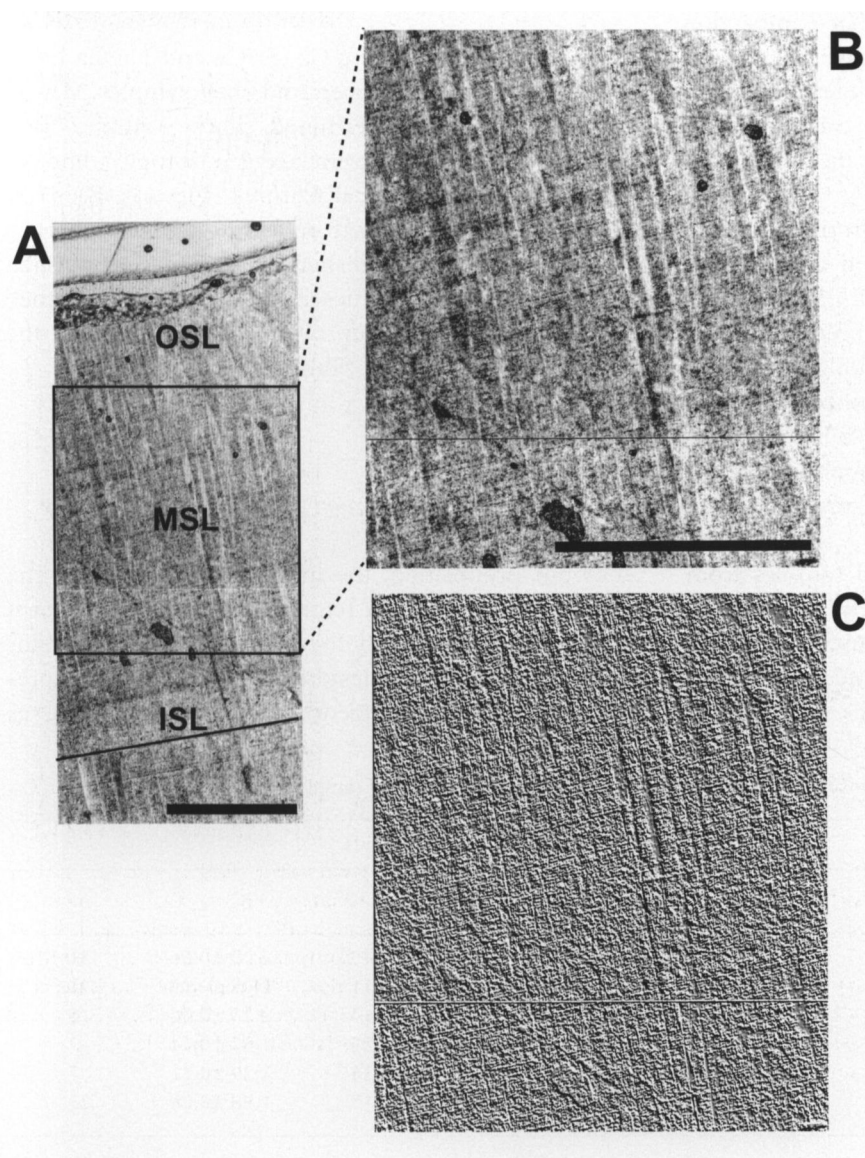

Fig. 4. Photomicrograph of inoceramid MA-33 (A); B shows detail of the MSL, while C is the same microphotograph but modified by image analysis to increase the contrast of the dark growth lines. Note the regularity in growth-band thickness.

cite prisms decrease in width from the inner shell layer (ISL) to the outer shell layer (OSL). Each inoceramid prism corresponds to a single or to various crystals and is about 0.1 mm (ISL) to 0.01 mm (OSL) wide and between 1 and 3 mm long. Alternating dark (*laminae obscurae*) and clear (*laminae pellucidae*) growth lines, commonly spaced at intervals of approximately 20 μm, are visible perpendicular to the long axes of the prisms and do not present any appreciable internal breaks (Fig. 4A-C). Lines gradually deflect towards the OSL. The calcite prisms are composed of low-magnesium calcite (LMC with < 4 mol% $MgCO_3$) and we did not observe the inner aragonitic nacreous shell layer described by other authors from other localities (Wright, 1987; Whittaker et al., 1987; Pirrie & Marshall, 1990).

For a detailed study under SEM and CL, we chose samples from the Sopelana I and Bidart sections since these are composed entirely of marl/marly-limestone alternations and turbidite beds are absent. Nevertheless, the Bidart alternations are less indurated than those of Sopelana I, which implies that compaction and secondary calcite precipitation have been more pervasive at the Sopelana I section. In fact, the loss of intra- and interprism porosity due to calcite cement precipitation is visible under SEM in inoceramid shells from the Sopelana I section (Fig. 3A, B). The calcitic prismatic layers of the shells from the Bidart section seem to be well preserved and without evidence of neomorphism. The ISL and OSL, perpendicular to the long axis of the prisms, seem to consist of regular, simple prismatic calcite, with a polygonal, honeycomb morphology and well-defined boundary surfaces (Fig. 3C, D). Very few calcite-filling cements can be observed between the prism boundaries. The microstructure of the individual prisms exhibits a uniformly distributed porosity.

Under CL, most of the inoceramid samples from the Sopelana I section show, in general, well-developed bright yellowish to red luminescence in the whole shell, and non-luminescent surfaces are absent (Fig. 6A). However, inoceramid shells from Bidart usually show a well-developed bright yellowish to red luminescence at shell edges and non-luminescent surfaces are visible in the middle shell layer (MSL) (Fig. 6B). Single inoceramid shell prisms floating in the sediment show a complete bright reddish to yellowish luminescence as well. Hendaya and Loya samples present high quantities of fracture-filling calcite cements with different luminescent behaviour (Fig. 3E-H).

Oxygen and carbon isotope values

The oxygen and carbon isotopes of a total of 244 samples (host-rock, n = 130; inoceramid shell prisms, n = 114) were determined. Isotopic results are given in Table 1. In shell prisms, the mean inoceramid oxygen and carbon isotope values were usually heavier than in host-rock (Fig. 5).

Inoceramid shell chemistry determined by electron microprobe

The Mg/Ca, Mn/Ca, Fe/Ca, Sr/Ca and Na/Ca ratios (mmol/mol) of the inoceramid shell samples MA-33 and BID-1 were determined. These samples were chosen due to their extreme oxygen isotopic compositions and petrographical features (Fig. 6A, B). Over 149 spots were analysed in sample MA-33 and 128 spots in the inoceramid shell BID-1. We distinguished between the non-luminescent and luminescent shell areas in order to set up chemical differences in the distribution both areas (Table 2; Fig. 6C-E).

Discussion

Inoceramid shell preservation and diagenetic behaviour

For our proposition, the inoceramid shells from the Bay of Biscay sections require that some of the form of their original morphological structure be found intact in marl/marly limestone couplets, and also preserve their pristine geochemical composition, as

Table 1. Mean oxygen and carbon isotope values from host-rock and inoceramid shells. n = number of samples analysed.

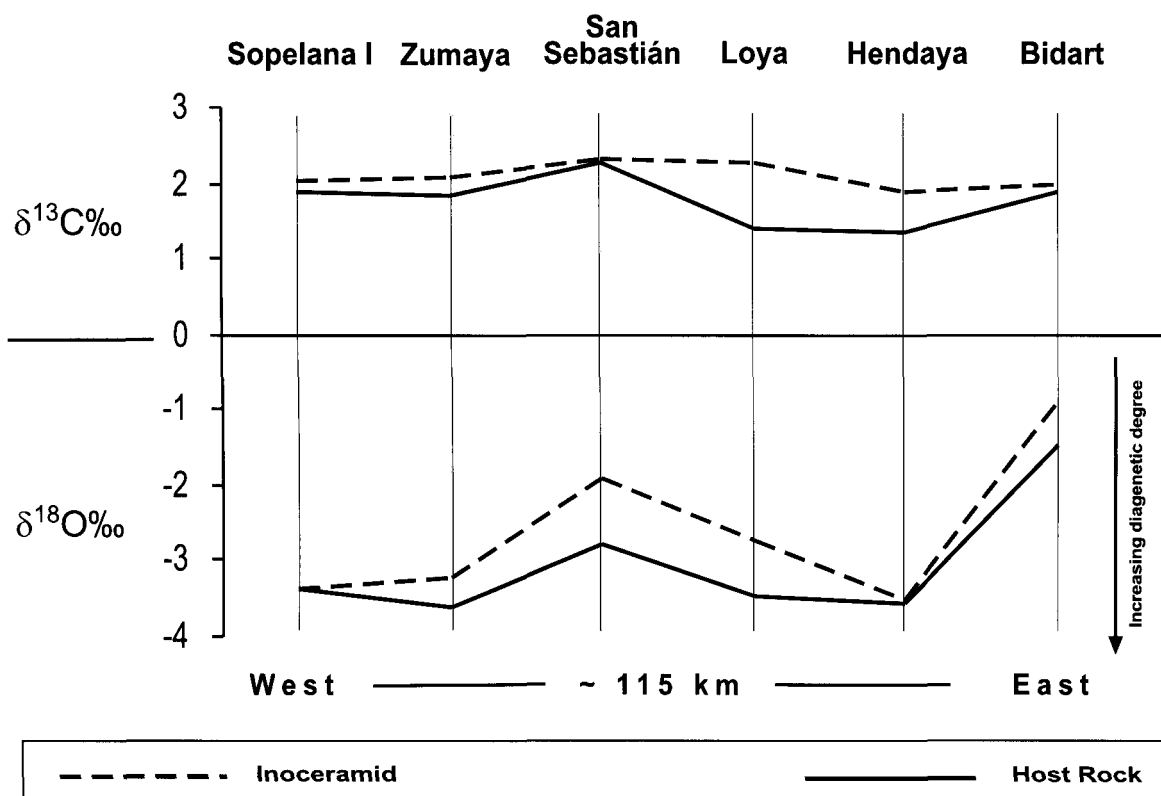|	Host Rock			Inoceramids		
	$\partial^{18}O$	$\partial^{13}C$	n	$\partial^{18}O$	$\partial^{13}C$	n
Sopelana I	-3,37 ±0,17	1,86 ±0,05	36	-3,36 ±0,10	2,04 ±0,06	31
Zumaya	-3,62 ±0,08	1,82 ±0,04	46	-3,24 ±0,11	2,07 ±0,05	41
San Sebastián	-2,79 ±0,05	2,26 ±0,04	6	-1,89 ±0,13	2,33 ±0,06	6
Hendaya	-3,58 ±0,11	1,37 ±0,11	7	-3,53 ±0,23	1,87 ±0,14	7
Loya	3,45 ±0,11	1,41 ±0,10	7	-2,74 ±0,14	2,29 ±0,11	7
Bidart	-1,46 ±0,22	1,89 ±0,03	28	-0,9 ±0,15	1,98 ±0,08	22

Fig. 5. Mean carbon and oxygen isotope values from inoceramid shells, together with host-rock samples, against spatial distribution of the studied Maastrichtian outcrops. Alpine orogeny folded the series and the ~115 km does not correspond to its original distance.

Brand & Morrison (1987) mentioned in their work on molluscs. However, oxygen and carbon isotope values from inoceramid shells and carbonate host-rock samples indicate clear diagenetic differences among the six sampled localities (Table 1). Mean oxygen isotope values, both in inoceramids and host-rock samples, tend to be lighter towards the western sections in response to increasing burial (Fig. 5; see also Fig. 1). The heaviest values correspond to the Bidart section whereas the lightest ones are found at Zumaya and Sopelana I. The Hendaya and Loya isotope values are similar to those found at Zumaya and Sopelana and disrupt this trend. As we have noted earlier, samples from the Hendaya and Loya sections present high quantities of fracture-filling calcite cements. Secondary calcite might be responsible for lowering the oxygen isotope signal.

The replacement of primary skeletal calcite and proteic matrix by secondary Fe-Mn rich calcite into intra and/or inter-prisms may be responsible for decreasing the oxygen isotope values of the inoceramid samples. In the same way, primary calcite dissolves in the carbonate host-rock, and is replaced by secondary calcite, which forms in equilibrium with the temperature and oxygen isotopic composition of carbonate sediment pore fluids. With increasing burial, the geothermal gradient elevates sediment temperatures and

the oxygen isotope values of secondary calcite should be more negative than those of the primary calcite. In contrast, carbon isotope values are not affected during diagenesis and they exhibit low variation between localities.

As Mii & Grossman (1994) and Grossman et al. (1996) noted, the distribution of minor and trace element contents in non-luminescent and luminescent areas of Pennsylvanian (Carboniferous) brachiopod shells was different. Consequently, we selected the two shells which had the lightest (MA-33, $\partial^{18}O$ = –5.18‰) and the heaviest (BID-1, $\partial^{18}O$ = –0.38‰) oxygen isotope values. During burial diagenesis, the composition of inoceramid shells has to change in order to reach the new chemical 'equilibrium conditions'. In this sense they obtain a trace element composition shifted towards equilibrium with the interstitial fluids, probably seawater in origin. The new inoceramid shell chemical composition was reached without any substantial change in the calcite prism microstructure, which suggests that element substitution took place atom by atom (solid-state diffusion).

This post-depositional element exchange produced chemical zoning in the shells (Table 2). Thus, luminescent and more altered shell areas became selectively enriched in Mn/Ca, Fe/Ca and Na/Ca and consequently lower Mg/Ca and Sr/Ca ratios (Fig. 6C, D).
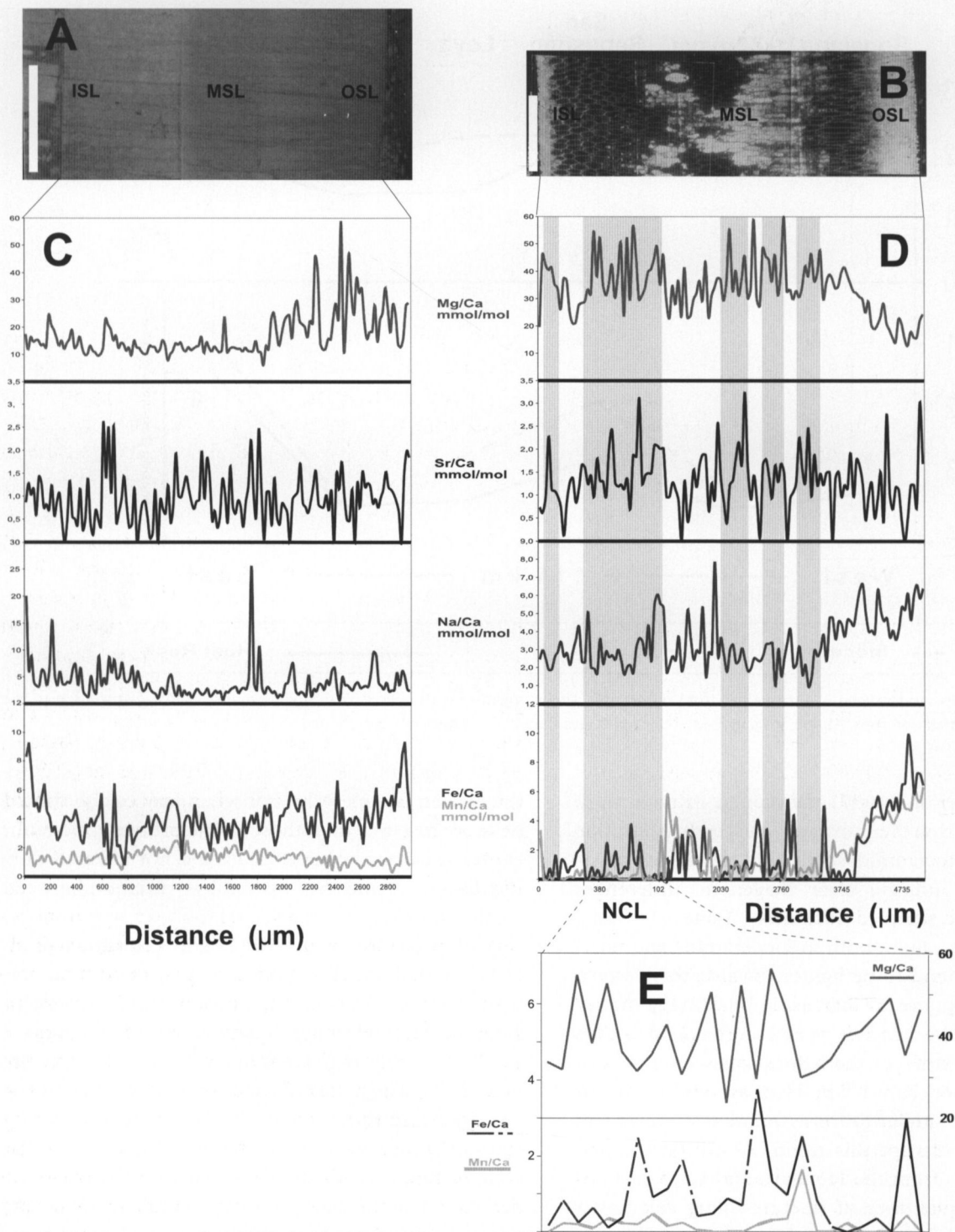
Fig. 6. MA-33 (A) and BID-1 (B) inoceramid shell CL photomicrographs. In contrast to that observed in the MA-33 shell (C), in the BID-1 inoceramid sample (D), two different trends in elemental composition for the non-luminescent (shaded areas) and luminescent areas (non-shaded areas) were detected. E shows the relationship among elemental ratios (see text for details). Optical magnification during chemical analysis limited the accuracy of spotting, but each spot approximately corresponds to a dark or clear growth band. Elemental ratios are given in mmol/mol.

On the other hand, low Mn/Ca, Fe/Ca and Na/Ca and well-correlated Mg/Ca and Sr/Ca ratios are found in non-luminescent (less altered) inoceramid shell areas (Fig. 6D). In general, diagenetic re-equilibria in a closed system (low water/rock ratio) may explain why the original oscillatory elemental distrib-

ution is partially preserved in the luminescent shells areas. Conversely, high water/rock ratios could lead to a more pervasive diagenesis with numerous dissolution-reprecipitation events (Brand & Veizer, 1980). Carbon isotope values suggest that re-equilibration of calcite with the surrounding diagenetic fluids took

Table 2. Mean elemental ratios along BID-1 and MA-33 shell profiles.
CL = luminescent areas; **NCL** = non-luminescent areas; **n** = number of analyses.

BID-1	$\partial^{18}O$	mmol/mol				
		Mg/Ca	**Sr/Ca**	**Na/Ca**	**Mn/Ca**	**Fe/Ca**
	-0,38					
Mean value; n=128		33,74	1,30	3,38	1,52	1,86
Mean value CL; n=52		26,02	1,16	4,02	2,99	3,08
Mean value NCL; n=76		39,02	1,40	2,94	0,51	1,02
MA-33	-5,18					
Mean value CL; n=149		17,19	0,93	4,02	1,34	4,01

place in a closed system (Emrich et al., 1970; Scholle & Arthur, 1980; Maliva et al., 1991).

In our case, as we have pointed out before, we observed a trend in element incorporation in both luminescent or non-luminescent areas, although a better compositional regularity characterises the BID-1 non-luminescent shell (Fig. 6D). We have noted that, although diagenetic processes tend to obliterate the primary biogenic calcite signal, the original composition of the alternating dark (*laminae obscurae*) and clear (*laminae pellucidae*) growth lines might control the amount of element exchange. The possibly primary Mg, Sr, Na, Fe and Mn values (as ppm) in non-luminescent sections of the inoceramid shell BID-1 could be inferred in the same way. These values nearly fall in the range of Mg, Sr, Na, Fe and Mn Cretaceous molluscan and bivalve LMC contents compiled by Ragland et al. (1979) and Brand & Morrison (1987) (Table 3).

Nutritionally controlled growth pattern

In bivalves and belemnite rostra, alternating clear and dark growth lines are interpreted as inorganic and organic-rich layers, respectively (Kennish, 1980; Sælen, 1989). It is well known that bivalve molluscs secrete shell material in periodic growth increments, which can provide a record of environmental conditions (productivity, temperature and salinity) during growth. Therefore, trace element distributions in shallow-water marine bivalves are often analysed, since

the shallow-marine environment is subject to a variety of changes in temperature and chemical conditions.

A detailed study of the clear and dark growth line arrangement, up to 500 in inoceramid sample MA-33, shows that they were commonly more densely packed in mature shell portions (ISL), without any observable internal breaks (Fig. 4), indicating a gradual decrease in growth rate throughout ontogeny. This closely spaced feature is a common characteristic in deep-sea bivalves (Gilkinson et al., 1986). In bivalves, dark organic-rich lines, now luminescent, are often correlated with seasonal events. In general, molluscs close their valves under adverse conditions, and have less or no contact with the surrounding water and therefore shell accretion decreases (Lutz & Rhoads, 1980; Barbin et al., 1991a, b; Barbin et al., 1995). The alternating dark and clear, regularly spaced growth lines suggest that shell accretion took place under stable and often changing environmental conditions.

As stenotopic organisms, deep-water ocean inoceramids probably did not experience strong environmental fluctuations (temperature and salinity) to produce similar skeletal Mg/Ca and Sr/Ca trends as found in shallow-water marine molluscs. Therefore, shallow-water, sessile, eurytopic molluscs might be sufficiently flexible to change their physiological system in response to changes in environmental conditions. Klein et al. (1996a, b) pointed out that the Mg/Ca ratios in shallow-water molluscan shells do not show a strong dependence on salinity but vary

Table 3. Comparative values among elemental contents in non-luminescent zones from the BID-1 inoceramid shell and compiled literature data on bivalves and other molluscs.

ppm	Bivalves LMC★	Upper Cretaceous★★	BID-1
Mg	860 - 9560	784 - 2216	9120
Sr	460 - 2700	637 - 1153	1178
Na	1630 - 4190	3507 - 4559	650
Fe	8 - 950	25 - 123	550
Mn	5 - 294	0 - 870	269

★ Brand & Morrison (1987)
★★Ragland et al. (1979). Gastropods and bivalves.

linearly with temperature alternations. The Sr/Ca ratio in skeletal calcite seems to be more closely related to mantle metabolic activity than to variations in seawater salinity. Klein et al. (1997) reported that the skeletal Sr/Ca ratio is positively correlated with seawater $\partial^{18}O$ values in mature parts of the shell, where the intracellular transport mechanism dominates, so in this shell portion, Mg/Ca (due to its positive relationship with temperature) and Sr/Ca should present similar trends.

On the other hand, Purton et al. (1999) found that temperature has only a secondary influence on Sr/Ca ratios on the Eocene aragonitic bivalve *Venericardia planicosta* and that metabolic factors can exert an important control. Carpenter & Lohmann (1992) pointed out that high Sr contents of biotic calcite result from rapid precipitation rates associated with shell accretion in a variety of Holocene marine phyla (Rhodophyta, Brachiopoda, Bryozoa, Echinodermata, Coelenterata and Protista) at different locations and depths and do not exclude the possibility that Mg incorporation may be a function of the precipitation rate. They also reported on the positive linear relationship of Sr and Mg contents of Holocene biotic marine calcite. Busenberg & Plummer (1985), in their study of calcites and selected aragonites, suggested that the amounts of Na incorporated in calcite vary as a function of the rate of crystal growth. Mii & Grossman (1994) found that Mg and Na contents of fossil brachiopod shells correlate inversely with $\partial^{18}O$ and pointed out that the Mg, Na concentrations increase with either increasing temperature or growth rate.

The behaviour of Mn and Fe, minor constituents in seawater, varies inversely with dissolved oxygen and correlates with nutrients (Kennish & Lute, 1994). Dromgoole & Walter (1990), in their study of calcite overgrowth, pointed out that Mn and Fe distribution coefficients increase with decreasing precipitation rates or increasing temperature. The manganese concentration in neritic benthic organisms also seems to be positively related to slow growth (Barbin et al., 1991a, b).

In our study, we found a consistent relationship among skeletal Mg/Ca and Sr/Ca ratios which are inversely related to Fe/Ca, Mn/Ca and Na/Ca ratios, suggesting that the primary palaeoenvironmental signal could be partially preserved in the non-luminescent areas of the BID-1 inoceramid shell (Fig. 6D, E). As temperature and salinity variations in deep-sea environments are minimal (Tyler, 1988) and light is absent, food (downward flux of phytodetritus) would appear to be the dominant factor for the inoceramid life cycle and the best candidate for controlling the

variation of Mg, Sr, Na, Fe and Mn during shell growth. The oscillatory curves of these elements along intrashell profiles could imply an annual/seasonal periodicity in inoceramid shell accretion.

The seasonal rain of phytodetritus is common in modern oceans both at high and low latitudes. Billett et al. (1983), studying the modern sedimentation of phytoplankton to deep-sea benthos, found a seasonal pulse of detrital organic material to bathyal and abyssal depths. This organic material seems to be derived directly from the source, i.e. primary production in surface-sea, and to sink rapidly to the deep-sea benthos. Considerable sedimentation of phytodetritus occurs soon after the spring bloom and continues throughout the early summer in temperate regions. Krantz et al. (1987), following the work of Heinrich (1962), also noted that in these regions, phytoplankton blooms occur during the spring as sunlight intensity increases or occasionally during the autumn in response to the mixing and nutrient replenishment associated with the deterioration of the thermocline. Tyler (1988) compiled published data on vertical seasonality flux in tropical domains. Seasonal flux of organic matter related to surface production has also been detected in tropical seas (Sargasso Sea, 32°5′ N), and may be associated with the presence of warmer-than-usual water in the top 500 m of the water column. Two periods of seasonal flux, in February-March and June-July have been detected at the Panama Basin (~5°N). The origin of this bimodal flux is related to upwelling periods (February-March) and phytoplankton blooms (June-July).

The phytodetritus rainfall towards the sea floor along continental margins probably constituted a seasonally enhanced food source for benthic inoceramid communities. Therefore, the geochemistry of the alternating dark and clear growth lines suggests that the growth pattern could be due to the input of seasonally controlled phytodetritus. If clear lines represent periods of 'rapid' growth or high mantle metabolic activity during phytodetritus settling, and dark ones indicate 'slower' growth when organic sedimentation decays, then a dark-clear line couple may represent one year in the inoceramid lifetime. But, if we consider two periods of phytodetritus rainfall, one year in the inoceramid life span is represented by two dark-clear couples. According to the total number of alternating dark and clear growth lines observed (≈500), the inoceramid life span could reach about 125 years in the case of two marked periods of organic matter settling, or 250 years, when considering a unique pulse of phytodetritus flux. This is not an anomalous age, since Turekian et al. (1975) determined by ^{228}Ra chronology that *Tindaria callistiformis*, a modern

deep-sea clam, reaches a length of 8.4 mm in about 100 years.

It is well known that the Cretaceous Period, a time of continuous climatic warmth with ice-free conditions, began to deteriorate towards colder temperatures during the Campanian-Maastrichtian interval and an increase equator to pole temperature gradients of 10 to 13EC (~0.4°C/1°) is calculated (see e.g., Barrera & Savin, 1999) and that the deterioration of the thermocline, enhanced by periodic changes in the water column, could be responsible for the seasonal variation in surface productivity. Also, sudden inputs of strontium resulting from the exposure of continental shelves and large positive oxygen isotope shifts (~1‰), coincident with dramatic short term sea-level falls, indirectly support the idea on the feasibility of periodic ice sheets in polar regions during the Cretaceous Period (Stoll & Schrag, 1996, 2000; Miller et al., 1999). Sea level falls and continent drift towards high latitudes affect the land-sea distribution which results in heat transport changes and, if so, seasonality (Crowley et al., 1986).

At the Bidart section, Clauser (1987), analysing bulk sediment, found a negative oxygen isotope excursion at the beginning of Member I superimposed on a period of marine regression. Gómez-Alday et al. (unpublished data) have found changes in stable isotope composition and clay mineralogy which affect Member I and Member II in the Sopelana I, Zumaya and Bidart sections which preclude distinct palaeoclimatic conditions. Inoceramids are abundant in these members, particularly in Member I, but are poorly represented at deeper levels and are absent above. This pattern of appearance indicates that inoceramids could survive under a narrow range of palaeoecological parameters. If progressive climate deterioration enhanced seasonality, with slight variations in annual subsurface temperatures and related changes in surface productivity, the expansion of temporary inoceramid benthic communities could have been favoured.

Conclusions

In the present study, we report that mid-Maastrichtian inoceramid shells from the Bay of Biscay sections show a lateral westward increase of their degree of diagenesis, without any substantial textural changes in the prismatic microstructure. This inference is made on the basis of measurements of $\partial^{18}O$, $\partial^{13}C$ and minor and trace element concentrations in inoceramid shells and marl/marly-limestone host-rock samples.

Progressive diagenesis caused a complete luminescent area in the inoceramid shell MA-33, from the Sopelana I section, and resulted in both an enrichment of Mn, Fe and Na values as well as a loss of Mg and Sr contents. Nevertheless, oscillatory curves, primary in origin, are still partially preserved due to low water/rock ratios (closed system). The loss of Mg is stronger than that of Sr giving a flattened trend in the luminescent area. In the non-luminescent shell areas, Mg, Sr, Na, Fe and Mn values are interpreted as being closer to the original primary values.

The lowest Mn, Fe and Na contents occur in the non-luminescent inoceramid shell area (BID-1, Bidart section) and Mg and Sr values are well correlated exhibiting a characteristic trend. This trend suggests that inoceramid shell accretion probably responded to changes in the calcite precipitation rate, which is related to seasonally pulsed phytodetritus. We estimate that the lifetime of some deep-water ocean inoceramid shells could be about 125 to 250 years. From a palaeoenvironmental point of view, the inoceramid acme appears to be related to Campanian-Maastrichtian climate change, which could have imprinted a marked seasonality.

Acknowledgements

References

Barbin, V., Ramseyer, K., Debenay, J.P., Schein, E., Roux, M. & Decrouez, D., 1991a. Cathodoluminescence of recent biogenic carbonates: an environmental and ontogenetic fingerprint. Geological Magazine 128: 19-26.

Barbin, V., Schein, E., Roux, M., Decrouez, D. & Ramseyer, K., 1991b. Stries de croissance révélées par cathodoluminescence dans la coquille de Pecten maximus (L.) récent de la Rade de Brest (Pectinidae, Bivalvia). Geobios 24: 65-70.

Barbin, V., Brand, U., Hewitt, R.A. & Ramseyer, K., 1995. Similarity in cephalopod shell biochemistry since Carboniferous: evidence from cathodoluminescence. Geobios 28: 701-710.

Barrera, E. & Tevesz, M.J.S., 1990. Oxygen and carbon isotopes: utility for environmental interpretation of recent and fossil invertebrate skeletons. In: Carter, J.G. (Ed.): Skeletal biomineralization: pattern and evolutionary trends. Van Nostrand (New York): 557-566.

Barrera, E., Tevesz, M.J.S. & Carter, J.G., 1990. Variations in oxygen and carbon isotopic compositions and microstructure of the shell of Adamussium colbecki (Bivalvia). Palaios 5: 149-159.

Barrera, E. & Savin, S.M., 1999. Evolution of late Campanian-Maastrichtian marine climates and oceans. In: Barrera, E. &

Johnson, C.C. (Eds): Evolution of the Cretaceous ocean-climate system. Geological Society of America, Special Paper 332: 245-282.

Barron, E.J., Saltzman, E. & Price, D.A., 1984. Occurrence of *Inoceramus* in the South Atlantic and oxygen isotopic palaeotemperatures in Hole 5300. Initial Reports of Deep Sea Drilling Project 75: 893-904.

Billett, D.S.M., Lampitt, R.S., Rice, A.L. & Mantoura, R.F.C., 1983. Seasonal sedimentation of phytoplankton to the deep-sea benthos. Nature 302: 520-522.

Brand, U. & Veizer, J., 1980. Chemical diagenesis of a multi-component carbonate system, 1: Trace elements. Journal of sedimentary Petrology 50: 1219-1236.

Brand, U. & Morrison, J.O., 1987. Biochemistry of fossil marine invertebrates. Geoscience Canada 14: 85-107.

Busenberg, E. & Plummer, L.N., 1985. Kinetic and thermodynamic factors controlling the distribution of SO_4^{-2} and Na^+ in calcites and selected aragonites. Geochimica et Cosmochimica Acta 49: 713-725.

Carpenter, S.J. & Lohmann, K., 1992 Sr/Mg ratios of modern marine calcite: empirical indicators of ocean chemistry and precipitation rate. Geochimica et Cosmochimica Acta 56: 1837-1849.

Clauser, S., 1987. Evolution de la composition isotopique de l'oxygène des carbonates durant le Campanien-Maastrichtien. Données préliminaires issues de la série de Bidart (Pyrénées Atlantiques). Comptes rendus de l'Académie des Sciences Paris (2)304(11): 579-584.

Crowley, T.J., Short, D.A., Mengel, J.G. & North, G.R., 1986. Role of seasonality in the evolution of climate during the last 100 million years. Science 231: 579-584.

Dauphin, Y., Gautret, P. & Cuif, J.P., 1996. Evolution diagénétique de la composition chimique des aragonites biogéniques chez les spongiaires, coraux et céphalopodes triasiques du Taurus lycien (Turquie). Bulletin de la Société géologique de France 167: 247-256.

Dhondt, A.V., 1992. Cretaceous inoceramid biogeography: a review. *In*: Malmgren, B.A. & Bengtson, P. (Eds): Biogeographic patterns in the Cretaceous ocean. Palaeogeography, Palaeoclimatology, Palaeoecology 92: 217-232.

Dickson, J.A.D., 1965. A modified staining technique for carbonates in thin section. Nature 205: 587.

Dodd, J.R. & Stanton, R.J., 1981. Palaeoecology. Concepts and applications. Wiley (Chichester): 559 pp.

Dromgoole, E.D. & Walter, L.M., 1990. Iron and manganese incorporation into calcite: effects of growth kinetics, temperature and solution chemistry. Chemical Geology 81: 311-336.

Elorza, J. & García-Garmilla, F., 1996. Petrological and geochemical evidence for diagenesis of inoceramid bivalve shells in the Plentzia Formation (Upper Cretaceous, Basque-Cantabrian Region, northern Spain). Cretaceous Reearch 17: 479-503.

Elorza, J. & García-Garmilla, F., 1998. Palaeoenvironmental implications and diagenesis of inoceramid shells (Bivalvia) in the mid-Maastrichtian beds of the Sopelana, Zumaya and Bidart sections (coast of the Bay of Biscay, Basque Country). Palaeogeography, Palaeoclimatology, Palaeoecology 141: 303-328.

Elorza, J., García-Garmilla, F. & Jagt, J.W.M., 1997. Diagenesis-related differences in isotopic and elemental composition of late Campanian and early Maastrichtian inoceramids and belemnites from NE Belgium: palaeoenvironmental implications. Geologie en Mijnbouw 75: 349-360.

Emrich, K., Ehhalt, D.H. & Vogel, J.C., 1970. Carbon isotope fractionation during the precipitation of calcium carbonate. Earth and Planetary Science Letters 8: 363-371.

Feuillée, P. & Rat, P., 1971. Structures et paléogéographies pyrénéo-cantabriques. *In*: Historie structurale du Golfe de Gascogne. Technip (Paris): V.1-1-V.1-48.

Gilkinson, K.D., Hutchings, J.A., Oshel, P.E. & Haedrich, R.L., 1986. Shell microstructure and observations on internal banding pattern in the bivalves *Yoldia thraciaeformis* Storer, 1938, and *Nuculana pernula* Müller, 1779 (Nuculanidae) from a deep-sea environment. The Veliger 29: 70-77.

Gómez-Alday, J.J. & Elorza, J., 1998. Incremento lateral hacia el Oeste del grado diagenético en el Maastrichtiense medio del Arco Vasco: evidencias en inocerámidos y roca encajante. Geogaceta 24: 151-154.

Gómez-Alday, J.J., García-Garmilla, F. & Elorza, J., 1998. Inocerámidos y belemnites en facies de la creta (Aquitania, Pays de Caux, NE Ardenas): diferente comportamiento frente a la diagénesis. Geogaceta 25: 91-94.

Grossman, E.L., Mii, H.S., Zhang, C. & Yancey, T.E., 1996. Chemical variation in Pennsylvanian brachiopod shells - diagenetic, taxonomic, microstructural, and seasonal effects. Journal of sedimentary Research 66: 1011-1022.

Heinrich, A.K., 1962. The life histories of plankton animals and seasonal cycles of plankton communities in the oceans. Journal du Conseil international d'Exploration du Mer 27: 15-24.

Henoc, J. & Tong, M., 1978. Automatisation de la microsonde. Journal of Microscopy, Spectroscopy and Electronics 3: 247-254.

Jones, D.S. & Quitmyer, I.R., 1996. Making time with bivalve shells: oxygen isotopes and season of annual increment formation. Palaios 11: 340-346.

Kennish, M.J., 1980. Shell microgrowth analysis. *Mercenaria mercenaria* as a type example for research in population dynamics. *In*: Rhoads, D.C. & Lutz, R.A. (Eds): Skeletal growth of aquatic organisms. Plenum Press (New York): 255-294.

Kennish, M.J. & Lute, P.L., 1994. Marine chemistry. *In*: Kennish, M.J. & Lute, P.L. (Eds): Practical handbook of marine science (2nd edition). CRC (Boca Raton): 566 pp.

Klein, R.T, Lohmann, K.C. & Thayer, C.W., 1996a. Bivalve skeletons record sea-surface temperature and $\partial^{18}O$ via Mg/Ca and $^{18}O/^{16}O$ ratios. Geology 24: 415-418.

Klein, R.T, Lohmann, K.C. & Thayer, C.W., 1996b. Sr/Ca and $^{13}C/^{12}C$ ratios in skeletal calcite of *Mytilus trossulus*: covariation with metabolic rate, salinity, and carbon isotopic composition of seawater. Geochimica et Cosmochimica Acta 60: 4207-4221.

Klein, R.T., Lohmann, K.C. & Kennedy, G.L., 1997. Elemental and isotopic proxies of paleotemperature and paleosalinity: climate reconstruction of the marginal northeast Pacific ca. 80 ka. Geology 25: 363-366.

Krantz, D.E., Williams, D.F. & Jones, D.S., 1987. Ecological and paleoenvironmental information using stable isotope profiles from living and fossil molluscs. Palaeogeography, Palaeoclimatology, Palaeoecology 58: 249-266.

Lutz, R.A. & Rhoads, D.C., 1980. Growth patterns within the molluscan shell: an overview. *In*: Rhoads, D.C. & Lutz, R.A. (Eds): Skeletal growth of aquatic organisms: biological records of environmental change. Plenum Press (New York): 203-254.

MacLeod, K.G., 1994. Extinction of inoceramid bivalves in Maastrichtian strata of the Bay of Biscay region of France and Spain. Journal of Paleontology 68: 1048-1066.

MacLeod, K.G. & Ward, P.D., 1990. Extinction pattern of *Inoceramus* (Bivalvia) based on shell fragment biostratigraphy. *In*: Sharpton, V.L. & Ward, P.D. (Eds): Global catastrophes in Earth history. Geological Society of America, Special Paper 247: 509-518.

MacLeod, K.G. & Orr, W.N., 1993. The taphonomy of Maastrichtian inoceramids in the Basque region of France and Spain and the pattern of their decline and disappearance. Paleobiology 19: 235-250.

MacLeod, K.G., Huber, B.T. & Ward, P.D., 1996. The biostratigraphy and paleobiogeography of Maastrichtian inoceramids. *In*: Ryder, G., Fastovsky, D. & Gartner, S. (Eds): The Cretaceous-Tertiary event and other catastrophes in Earth history. Geological Society of America, Special Paper 307: 361-373.

Maliva, R.G., Dickson, J.A.D. & Räheim, A., 1991. Modelling of chalk diagenesis (Eldfisk Field, Norwegian North Sea) using whole rock and laser ablation stable isotopic data. Geological Magazine 128: 43-49.

Mann, K.O., 1992. Physiological, environmental, and mineralogical controls on Mg and Sr concentrations in *Nautilus*. Journal of Paleontology 66: 620-636.

Mathey, B., 1982. El Cretácico superior del Arco Vasco. *In*: Universidad Complutense (Ed.): El Cretácico de España. Universidad Complutense (Madrid): 111-136.

Mathey, B., 1987. Les flyschs crétacés supérieur des Pyrénées basques. Mémoires géologiques de l'Université de Dijon 12: 142-147.

McCrea, J.M., 1950. On the isotopic chemistry of carbonates and a paleotemperature scale. Journal of Chemistry and Physics 18: 669-673.

Mii, H.S. & Grossman, E.L., 1994. Late Pennsylvanian seasonality reflected in the ^{18}O and elemental composition of a brachiopod shell. Geology 22: 661-664.

Miller, K.G., Barrera, E., Olsson, R.K. & Savin, S.M., 1999. Does ice drive early Maastrichtian eustasy? Geology 27: 783-786.

Morrison, J.O. & Brand, U., 1984. Secular and environmental variation of seawater: an example of brachiopod chemistry. Geological Association of Canada, Annual Meeting, Programme and Abstracts 9: 91.

Morrison, J.O. & Brand, U., 1986. Geochemistry of recent marine invertebrates. Geoscience Canada 13: 237-254.

Morrison, J.O. & Brand, U., 1988. An evaluation of diagenesis and chemostratigraphy of Upper Cretaceous molluscs from the Canadian Interior Seaway. Chemical Geology (Isotope Geoscience Section) 72: 235-248.

Pirrie, D. & Marshall, J.D., 1990. Diagenesis of Inoceramus and Late Cretaceous paleoenvironmental geochemistry: a case study from James Ross Island, Antarctica. Palaios 5: 336-345.

Pujalte, V., Baceta, J.I., Orue-Etxebarria, X. & Payros, A., 1998. Paleocene strata of the Basque Country, western Pyrenees, northern Spain: facies and sequence development in a deep-water starved basin. *In*: Graciansky, P. de, Hardenbol, J., Jacquin, T. & Vail, P. (Eds): Mesozoic and Cenozoic sequence stratigraphy of European basins. Society of Economic Petrologists and Mineralogists, Special Publication 60: 311-325.

Purton, L.M.A., Shields, G.A., Brasier, M.D. & Grime, G.W., 1999. Metabolism controls Sr/Ca ratios in fossil aragonitic mollusks. Geology 27: 1083-1086.

Ragland, P.C., Pilkey, O.H. & Blackwelder, B.W., 1979. Diagenetic changes in the elemental composition of unrecrystallized mollusk shells. Chemical Geology 25: 123-134.

Rat, P., 1959. Les Pays crétacés basco-cantabriques. Publications de l'Université de Dijon 18: 1-525.

Sælen, G., 1989. Diagenesis and construction of the belemnite rostrum. Palaeontology 32: 765-798.

Saito, T. & Van Donk, J., 1974. Oxygen and carbon isotopic measurements of Late Cretaceous and Early Tertiary foraminifera. Micropaleontology 20: 152-177.

Saltzman, E.S. & Barron, E.J., 1982. Deep circulation in the Late Cretaceous: oxygen isotope paleotemperatures from *Inoceramus* remains in DSDP cores. Palaeogeography, Palaeoclimatology, Palaeoecology 40: 167-181.

Scholle, P.A. & Arthur, M.A., 1980. Carbon isotope fluctuations in Cretaceous pelagic limestones: potential stratigraphic and petro-

leum exploration tool. American Association of Petroleum Geologists Bulletin 64: 67-87.

Stoll, H.M. & Schrag, D.P., 1996. Evidence for glacial control of rapid sea level changes in the Early Cretaceous. Science 272: 1771-1774.

Stoll, H.M. & Schrag, D.P., 2000. High-resolution stable isotope records from the Upper Cretaceous rocks of Italy and Spain: glacial episodes in a greenhouse planet?. Geological Society of America Bulletin 112: 308-319.

Turekian, K.K., Cochran, J.K., Kharkar, D.P., Cerrato, R.M., Vaisnys, J.R., Sanders, H.L., Grassle, J.F. & Allen, J.A., 1975. Low growth rate of a deep-sea clam determined by ^{228}Ra chronology. Proceedings of the national Academy of Sciences (USA) 72: 2829-2832.

Tyler, P.A., 1988. Seasonality in the deep sea. Oceanographic Marine Biology Annual Review 26: 227-258.

Veizer, J., Fritz, P. & Jones, B., 1986. Geochemistry of brachiopods: oxygen and carbon isotopic records of Paleozoic oceans. Geochimica et Cosmochimica Acta 50: 1679-1696.

Ward, P.D., Kennedy, W.J., MacLeod, K.G. & Mount, J., 1991. End-Cretaceous molluscan extinction patterns in Bay of Biscay K/T boundary sections: two different patterns. Geology 19: 1181-1184.

Ward, P.D. & Kennedy, W.J., 1993. Maastrichtian Ammonites from the Biscay Region (France, Spain). Paleontological Society Memoir 34: 1-58.

Whittaker, S.G., Kyser, T.K. & Caldwell, W.G.E., 1987. Palaeoenvironmental geochemistry of the Clagget marine cyclothem in south-central Saskatchewan. Canadian Journal of Earth Sciences 24: 967-984.

Wright, E.K., 1987. Stratification and paleocirculation of Late Cretaceous Western Interior Seaway of North America. Geological Society of America Bulletin 99: 480-490.